

Interacting domains in the epithelial sodium channel that mediate proteolytic activation

Jonathan M Berman, Ryan G Awayda, and Mouhamed S Awayda*

Department of Physiology and Biophysics; State University of New York at Buffalo; Buffalo NY USA

Keywords: activity, ENaC, furin, proteolysis, subtilisin, structure-function, trypsin

Epithelial Sodium Channel (ENaC) proteolysis at sites in the extracellular loop of the α and γ subunits leads to marked activation. The mechanism of this effect remains debated, as well as the role of the N- and C-terminal fragments of these subunits created by cleavage. We introduced cysteines at sites bracketing upstream and downstream the cleavage regions in α and γ ENaC to examine the role of these fragments in the activated channel. Using thiol modifying reagents, as well as examining the effects of cleavage by exogenous proteases we constructed a functional model that determines the potential interactions of the termini near the cleavage regions. We report that the N-terminal fragments of both α and γ ENaC interact with the channel complex; with interactions between the N-terminal γ and the C-terminal α fragments being the most critical to channel function and activation by exogenous cleavage by subtilisin. Positive charge modification at a.a.135 in the N-terminal fragment of γ exhibited the largest inhibition of channel function. This region was found to interact with the C-terminal α fragment between a.a. 205 and 221; a tract which was previously identified to be the site of subtilisin's action. These data provide the first evidence for the functional channel rearrangement caused by proteolysis of the α and γ subunit and indicate that the untethered N-terminal fragments of these subunits interact with the channel complex.

Introduction

The Epithelial Na^+ Channel (ENaC) is expressed in the collecting duct (CD) of the kidneys where it mediates regulated Na^+ absorption. It is a well-established rate limiting step to nephron Na^+ absorption which ultimately can affect whole body Na^+ balance both in control and disease states.¹ Despite being initially cloned in 1993 and 1994,^{2–4} there remains a lack of structural data that underlie changes of channel function and activity. The best such data come from homology modeling of ENaC to a distantly related ion channel- ASIC1.⁵ The solved crystal structure of chicken ASIC1 has been used to create static images of ENaC subunits and to allow specific testable hypotheses for the role of domains identified from this modeling.^{6,7} This approach while informative suffers many shortcomings including: 1) the static nature of the ASIC model, 2) the low ~35% amino acid homology of ENaC to ASIC1, and the homomeric ASIC versus heteromeric nature of ENaC subunits which display only 30–40% homology,⁸ and 3) the absence of cleavage region found in α and γ from ASIC protein.

A unique mechanism that markedly increases ENaC activity involves cleavage of the α and γ subunits at multiple sites within a short (<40 a.a.) tract in their large extracellular loop.^{9,10} This process is endogenously and intracellularly carried out by furin type proteases.⁹ It is also mimicked by many extracellular proteases which activate membrane resident but electrically silent

uncleaved channels leading to dramatic activation of Na^+ transport.^{11–13}

When cleavage occurs it divides the α and γ subunits into 2 or more regions. Mechanism of cleavage activation is uncertain and 2 hypotheses have been proposed. The first was based on the presence of 2 initially identified endogenous cleavage sites in α and γ and the observation that short peptides with sequences derived from the amino acids between these “furin” sites inhibited activity when added exogenously.^{14,15} This hypothesis does not account for the presence of multiple identified and putative cleavage sites in these subunits, and the similarity of activation by cleavage observed with numerous exogenous proteases with different substrate specificities.¹⁶ We proposed the second hypothesis to explain activation based on: 1) the preservation of cleavage activation in the presence of a single cleavage event, 2) the preservation of cleavage activation in constructs lacking the “inhibitory” tracts, and 3) the much lower density of the N- to C-terminal fragments at the membrane. We proposed that activation is likely mediated by the loss of the 1st transmembrane domain following cleavage leading to a more stable channel possibly by reduction of hydrophobic mismatch between the channel and lipid bilayer.¹⁶

While data exist supporting both hypotheses, there is no clear indication for the mechanism of activation from existing structural models. The distantly homologous ASIC lacks corresponding “furin” sites and does not display proteolytic activation. Also,

*Correspondence to: Mouhamed S Awayda; Email: awayda@buffalo.edu

Submitted: 07/07/2015; Revised: 07/08/2015; Accepted: 07/10/2015

<http://dx.doi.org/10.1080/19336950.2015.1073869>

the region surrounding the endogenous furin cleavage sites in α and γ ENaC fall within what has been referred to as a “hypervariable region”⁶ of the extracellular loop, and is completely absent from ASIC. Moreover, in order to crystallize ASIC, the intracellular N- and C- termini were removed further diminishing the extrapolation to ENaC activation and the role of the 1st transmembrane domain in this activation. This is an important limitation as it is now known that intracellular channel domains can affect extracellular events such as proteolysis.^{17,18}

To better understand the dynamic structural events that occur with cleavage we used cysteine mutagenesis of sites of interest

and acutely modified these sites to determine their effect on exogenous cleavage. We focused our approach on the new termini formed by cleavage in α and γ ENaC. We engineered cysteines into these subunits in regions bracketing the “hypervariable” region. Using this approach and the exogenous protease subtilisin which cleaves within 16 a.a. downstream of furin,¹⁶ we identified multiple interactions between both fragments of cleaved γ and the C-terminal fragment of α ENaC which are important to cleaved channel function. Modification to γ at a.a.135 prior to the 1st furin cleavage exhibited the largest inhibition of channel activation by acute proteolysis. Insertion of a positive charge at

this position also inhibited the endogenously cleaved channel by ~98% and this inhibition was relieved by downstream cleavage by subtilisin. These, as well as other interactions converged on a tract in α downstream of the 2nd furin site in the new N-terminus of the C-terminal fragment between a.a. 205 and 221. We propose a refined hybrid model in which untethering of α and γ N-termini allows their interaction with the C-terminal fragment of α and the formation of an electrically active mature channel.

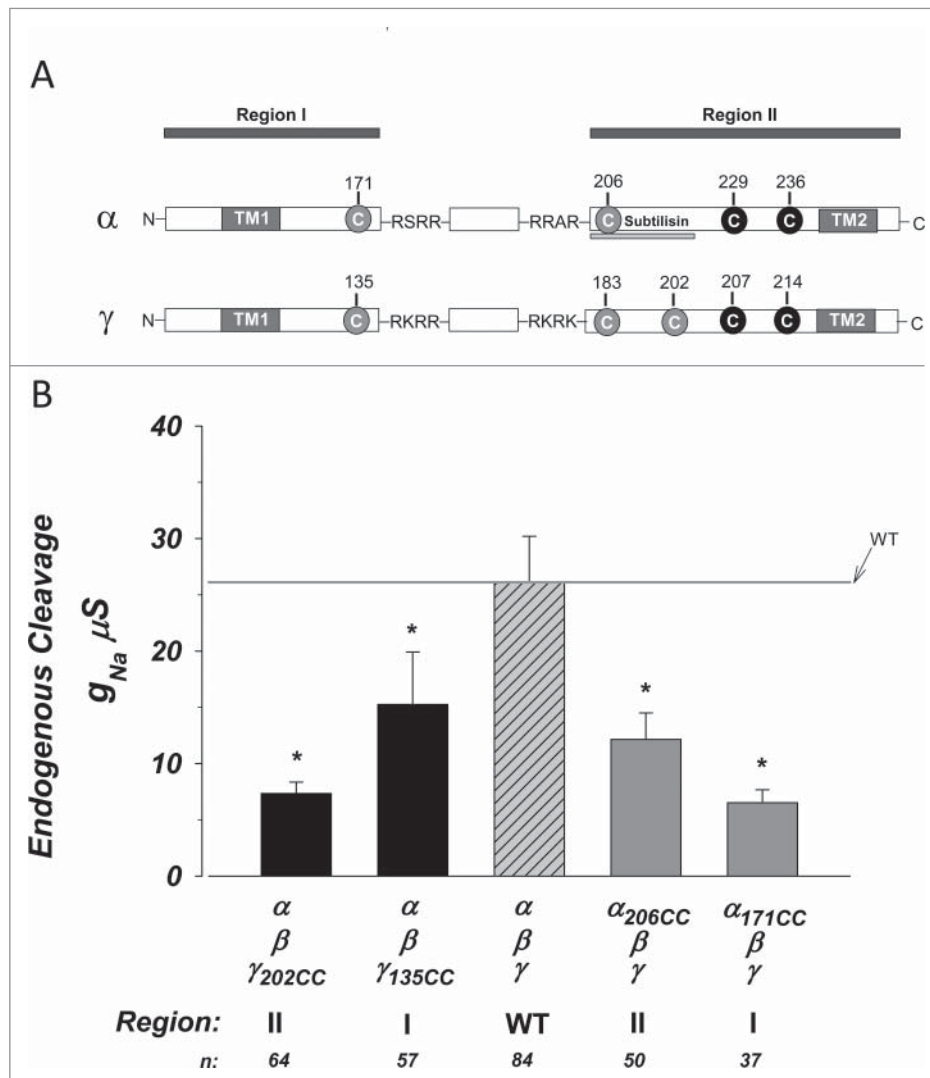


Figure 1. Exogenous cysteines bracketing the furin cleavage sites in α and γ ENaC reduce baseline activity. Constructs were created containing cysteines bracketing the furin cleavage sites in α and γ ENaC. (A) Linear graphic representation of the sites of exogenous cysteines (gray circles) relative to the furin cleavage sites (4 sequence amino acids), as well as nearby endogenous cysteines (black circles). The subunits were divided into regions I and II based on the segment prior to the first cleavage and that following the second cleavage. The site cleaved by subtilisin is underlined. TM1 and TM2 indicate the 2 transmembrane domains. (B) Summary of the amiloride sensitive slope conductance at 0 mV. The magnitude of conductance was significantly lower in each construct compared to wild type control. * indicates $P < 0.05$. N = 37–84.

Results

Baseline activity

Intracellular cleavage in oocytes occur at sites similar to those found in other cells at RSRR and RRAR in α ENaC and RKRR and RKRK in γ ENaC.⁹ We engineered cysteines to bracket these regions. A schematic representation is shown in Figure 1a. In this linear model we refer to the region produced prior to the first cleavage site as I, and that produced after the second cleavage site as II. The exogenous cysteines were introduced at VA171 and VA206, prior to “RSRR,” and after “RRAR” in α ENaC. Cysteines were introduced at 3 locations in γ at: 1) 135 prior to RKRR the first furin cleavage site, 2) GG183 after RKRR the second furin cleavage site, and 3) VG202 slightly downstream of the 2nd site and at a similar location to that marking the end of the subtilisin cleavage tract in α .¹⁶ The changes with VG202 were larger than those observed with GG183 and for clarity purposes the data with GG183 are not shown.

The baseline activity of the 4 constructs is shown in **Figure 1b**. We summarized activity as the amiloride sensitive conductance (g_{Na}) which average $26.1 \pm 4.0 \mu S$ for WT. The g_{Na} of all constructs was significantly lower than that of WT exhibiting a 2–4-fold inhibition indicating effects of the exogenous cysteines. Because the added cysteines are either upstream or downstream of cleavage, and because they are also displaced by up to 20 amino acids from the terminal cleavage amino acid (for VG202), it is likely that this inhibition is due to modification of activity and not large effects on endogenous cleavage. Nonetheless, this was tested biochemically.

To test for differences in protein expression, membrane density and endogenous cleavage we utilized Western Blotting using a C-terminal epitope γ specific antibody or a high affinity anti-HA antibody to detect double tagged (tagged in regions I and II) α . Mature (proteolytically cleaved) γ ENaC (**Fig. 2A**) was the dominant and often the only observed form. This product migrated at 55 kDa. In 1 of 4 blots (shown in the example) a very faint full length product was visible at ~ 75 kDa, and this constituted $<5\%$ of cleaved γ levels. This is consistent with our previous report that essentially only cleaved γ is observed at the membrane of trimeric ENaC expressing oocytes.¹⁶ As shown in **Figure 2B** there was no statistically significant difference in membrane expression of cleaved γ between constructs. These indicate that the effects on the g_{Na} observed in **Figure 1** were not due to differences in γ protein expression or its endogenous steady state cleavage.

Western Blotting for α ENaC is shown in **Figure 2C and D**. α was tagged with 2 separate HA tags to allow visualization of full length and fragments I and II with the same antibody using the same epitope as previously described.¹⁶ Biotinylated α protein migrated as 2 well defined bands at ~ 80 kDa and ~ 60 – 55 kDa, representing full and cleaved (region II) products. There was also a faint but consistent band at 24 kDa representing region I. As previously reported and as shown in **Figure 2C**, the 24 kDa product was much lower in intensity than that at 60 kDa. Combining cleaved and uncleaved, there was no statistically significant difference in α ENaC membrane levels among the different constructs (**Fig. 2D**).

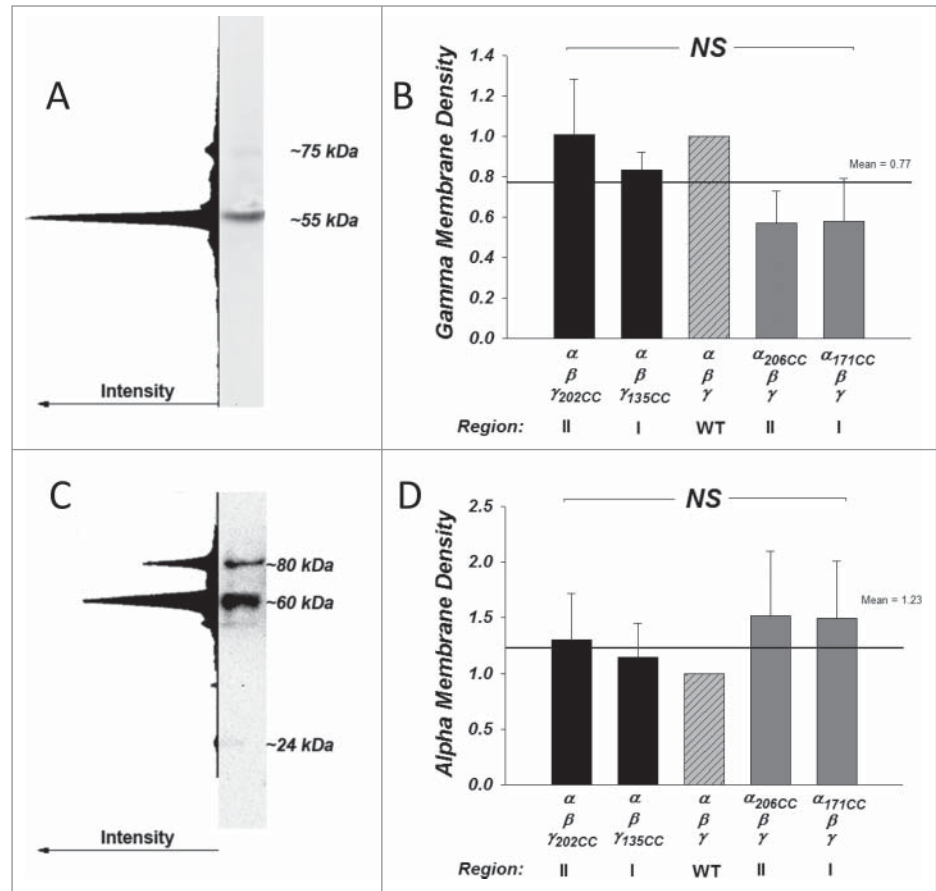


Figure 2. Subunit expression and processing is unchanged with exogenous cysteines. Membrane expression and endogenous cleavage of the γ and α subunits was examined by SDS-PAGE and Western Blot. **(A)** A representative blot demonstrating that virtually all of γ appeared as a single cleaved form at 55 kDa (region II) with little to no appearance of the full form at 75 kDa. This example was purposely chosen to represent the one showing the highest 75 kDa expression. This is confirmed by the intensity profile of the entire lane. **(B)** γ expression was measured by densitometry and normalized to WT. No differences were observed among all groups (NS = not significant) indicating absence of effects on expression and processing. Line and numerical mean represent the average of all groups. N = 3–5. **(C)** A representative blot shows the pattern of expression in the α subunit. α appeared as at least 2 distinct bands at 80 and 60 kDa, representing the full length and region II protein. The small region I band was barely detectable and migrated at 24 kDa. This detection was feasible because α contained 2 HA tags one each in regions I and II (see Methods). **(D)** α expression was measured by densitometry and normalized to WT. Summarized data represent the sum of cleaved and uncleaved protein. Overall, the expression was not different among all groups (NS = not significant) indicating absence of effects on expression. Line and numerical mean represent the average of all groups. N = 5–9.

The fraction of endogenously cleaved α at the membrane was unaffected (**Fig. S1**) by cysteine insertion. Further, there was no detectable shift in the size of the cleaved products which averaged 79 ± 2 , 56 ± 1 , and 24 ± 1 kDa for full, region II and region I products. These data rule out an effect of the exogenous cysteines on protein expression or membrane delivery for both α and γ subunits as the underlying effect causing changes of g_{Na} . This indicates that the inhibition observed in **Figure 1** is likely due to interactions of the exogenous cysteines in regions I and II in both α and γ with the trimeric conducting channel, i.e., the endogenously cleaved channel.

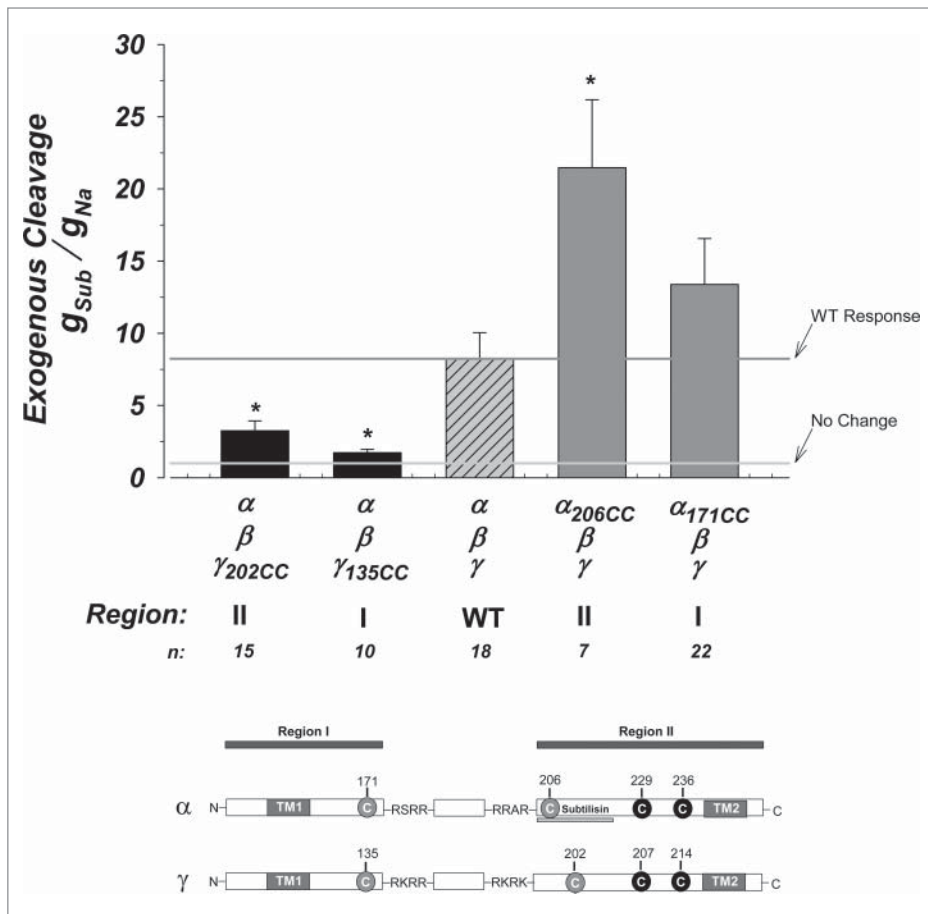


Figure 3. Activation of ENaC by subtilisin is altered by exogenous cysteines. Activation of ENaC constructs by subtilisin. Data were normalized to the control measured in each construct prior to the addition of this protease. All conductance ratios used the amiloride sensitive conductance which was obtained before and after subtilisin. On average, an 8-fold activation is observed in WT channels. Activation of γ region I and II were inhibited from WT while that in α region I was not affected. Activation of α region II was stimulated from WT by more than an additional 2-fold (8-fold vs. 21-fold). The horizontal lines represent the average response of the WT channel (dark gray) and a no change response. * indicates $P < 0.05$. $N = 7-22$. Linear model at bottom replotted from **Figure 1**.

Exogenous proteolysis

The data above allow an assessment of the steady-state effects of cysteine modification on channel activity following endogenous cleavage. To determine the acute effects of proteolysis we exogenously cleaved ENaC with the proteases subtilisin and trypsin. Subtilisin cleaves in a region slightly downstream of RRAR in α resulting in a region II that is very similar to that endogenously observed. Additional advantages of subtilisin are that: 1) it exhibits a higher sequence specificity than trypsin,¹⁹ 2) it does not affect endogenous protease activated receptors,¹⁶ and 3) unlike trypsin it lacks cysteines which make this enzyme stable and unaffected by the cysteine modifying reagents used in this study.

The effects of subtilisin are shown in **Figure 3**. The WT channel exhibited an 8.22 fold stimulation of g_{Na} consistent with that previously described.¹⁶ Examination of the effects of the cysteine mutants yielded 3 different results. First, there was no difference

between α 171CC and WT indicating that α region I does not interfere with subtilisin cleavage on α . This also indicates that the inhibition observed in **Figure 1** by this engineered cysteine is maintained when α is exogenously cleaved by subtilisin, meaning that region I in α interacts outside of the tract cleaved by subtilisin. Second, a stimulation was observed when comparing α 206CC vs. WT. This nearly 3-fold stimulation (21.47 fold vs 8.22 fold) indicates that elimination of the exogenous cysteines in this α region II by subtilisin led to stimulation of activity. In this case α 206 inhibits activity (**Fig. 1**) and its removal eliminates this inhibition. This indicates that this location in α may control activity of the mature channel- a hypothesis borne out by additional results below.

The third effect observed was a marked reduction in the activation by subtilisin in modifications of regions I and II in γ . Channels made with γ 202CC and γ 135CC were diminished from activation and exhibited only a 3.25 and 1.72 fold increase. This indicates that these regions are important for the activity of the mature and active channel and moreover, that they can modify the ability of subtilisin to cleave α in region II. As we have previously shown that subtilisin cleaves α between a.a. 205–221,¹⁶ these data indicate that the termini in γ regions I and II likely interact with α region II at this tract. These effects were similar whether subtilisin or trypsin (**Fig. S2**) was used to

cleave and activate ENaC. This further supports the interpretation that cysteines at these regions affect endogenously cleaved channel activity and that cleaved regions I and II in γ present likely points of contact with region II of α .

Thiol modification and charge

The exogenous cysteines represent points which can be acutely modified by thiol modifying reagents. Prior to these experiments, we determined if these cysteines remained unpaired and therefore accessible to such modification. Initially we examined the effects of 2 reducing agents: DTT and TCEP. Given the similarity of the initial data we focused on the stronger reducing agent TCEP. These effects are summarized in **Figure 4**. The WT channels exhibited a 40% reduction of activity indicating a likely effect on endogenous disulfides. γ constructs in region I and II behaved exactly as WT. This indicates that no new spontaneous disulfides are formed with the introduced cysteines. Similarly, no

differences from WT were also observed in the response of cysteines in α region II. Thus, these cysteines are expected to be amenable to thiol modification.

Reduction of cysteines in α region I were not affected by TCEP. This indicates possible stabilization compared to the WT channel which ends up protecting against the actions of TCEP on endogenous disulfides. This could be through the formation of a stabilizing new disulfide between an endogenous cysteine and those introduced at $\alpha 171$. Such an interpretation would be consistent with the absence of an effect of $\alpha 171$ on the stimulation by subtilisin (see Fig. 3), as the new cysteine are not available to interfere with subtilisin. This indicates that exogenous cysteines in $\alpha 206$, $\gamma 135$, and $\gamma 202$ are likely unpaired, while that in $\alpha 171$ is likely paired. These data also support the above conclusion that α region I is retained as part of the mature channel complex, as it can stabilize the disruption of other endogenous disulfide bridges in the active and furin cleaved channel.

To further determine the role of the termini in regions I and II we covalently modified them by positive and negative charges. We used MTSEA²⁰ to introduce a positive charge and MTSES²¹ to introduce a negative charge. Both molecules are relatively small (~20 Å on the long axis) allowing diffusability to exposed cysteines and the formation of strong sulfhydryl bonds with free cysteines resulting in charge modification. The effects of treatment with the positively charged MTSEA are shown in Figure 5. The WT channel was inhibited by ~38%. Addition of positive charge to γ in regions I and II were further inhibited from WT, although only that in γ region I was significant, where it was inhibited by ~98%. This provides strong evidence that γ region I remains associated and important to mature channel function.

Modifications to α regions I and II were not different from WT. This is expected for α region I as these cysteines were likely unavailable for modification. The lack of differences for α region II possibly indicates that the inhibition of baseline activity at this position is charge independent. Altogether, these results support a dominant role of region I in γ in mature channel activity and indicate that the order of potency for interactions with α region II are $\gamma 135 \gg \gamma 202 > \alpha 171$.

Treatment with negatively charged MTSES was without effect on all constructs and minimally affected $\alpha 135CC$ indicating a unique role of positive charges in this process

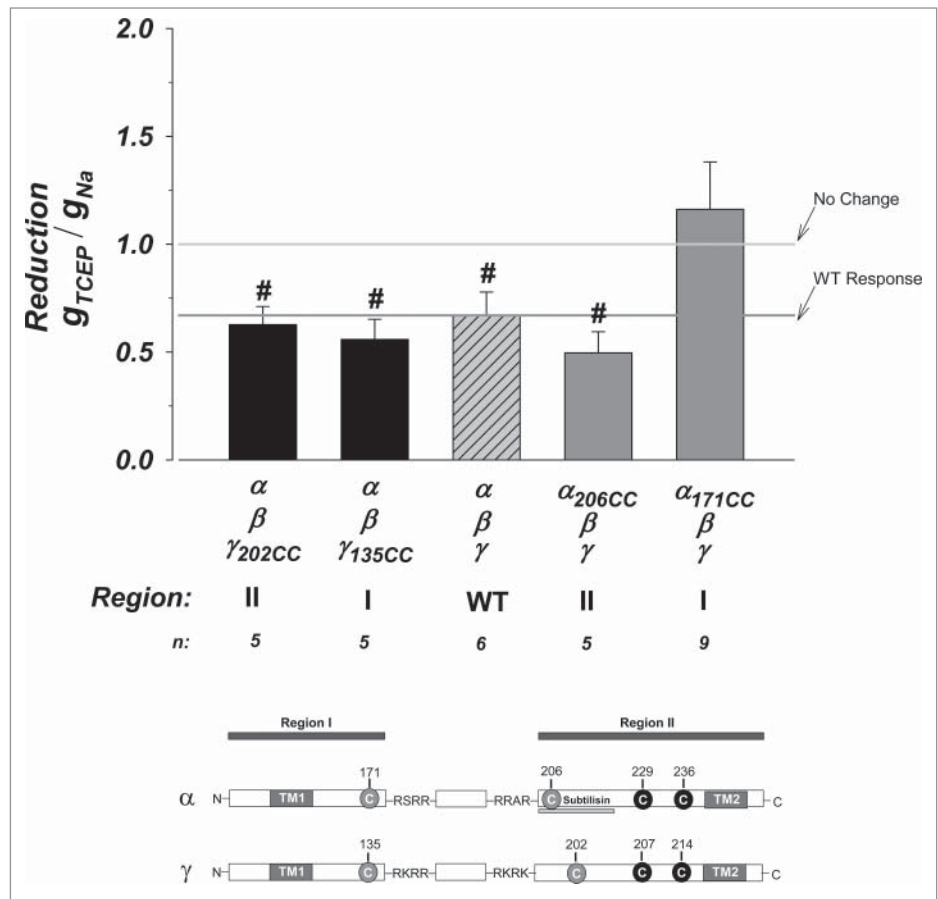


Figure 4. Effects of reduction on the cysteine mutant constructs. The strong reducing agent TCEP was used. This resulted in a small 40% inhibition of the WT channel. Constructs in α region II and γ regions I and II behaved as WT indicating no additional disulfides were formed by the introduced exogenous cysteines. Those in α region I were stimulated from WT and not different from no change indicating likely stabilization of the channel. N = 5–9. # indicates $P < 0.05$ when compared to no change. See Figure 3 legend for more details.

(Fig. S3). This indicates a more disruptive role of introducing positive charges than negative ones, and provides an interesting possibility for interactions with the positively conducted ion (see Discussion).

The effects of MTSEA occurred in electrically active channels and likely represent modification of subunits endogenously cleaved by furin-type intracellular proteases. Because of the role of subtilisin, many of the interactions described were pinpointed to region II in α between a.a. 205 and 221. To further ascertain this, we determined if subtilisin cleavage and elimination of this region can disrupt thiol modification. Subtilisin lacks cysteines and therefore it is unlikely to be affected by TCEP. This was also experimentally verified using 3 substrates with sequences that represent putative furin cleavage sites on ENaC: RTAR, RKRR, and RKRK. In this case treatment with 10-fold higher concentrations of TCEP (5 mM vs. 500 μ M) did not inhibit enzyme activity and only caused a moderate <2-fold stimulation to the activity to some substrates (Fig. S4).

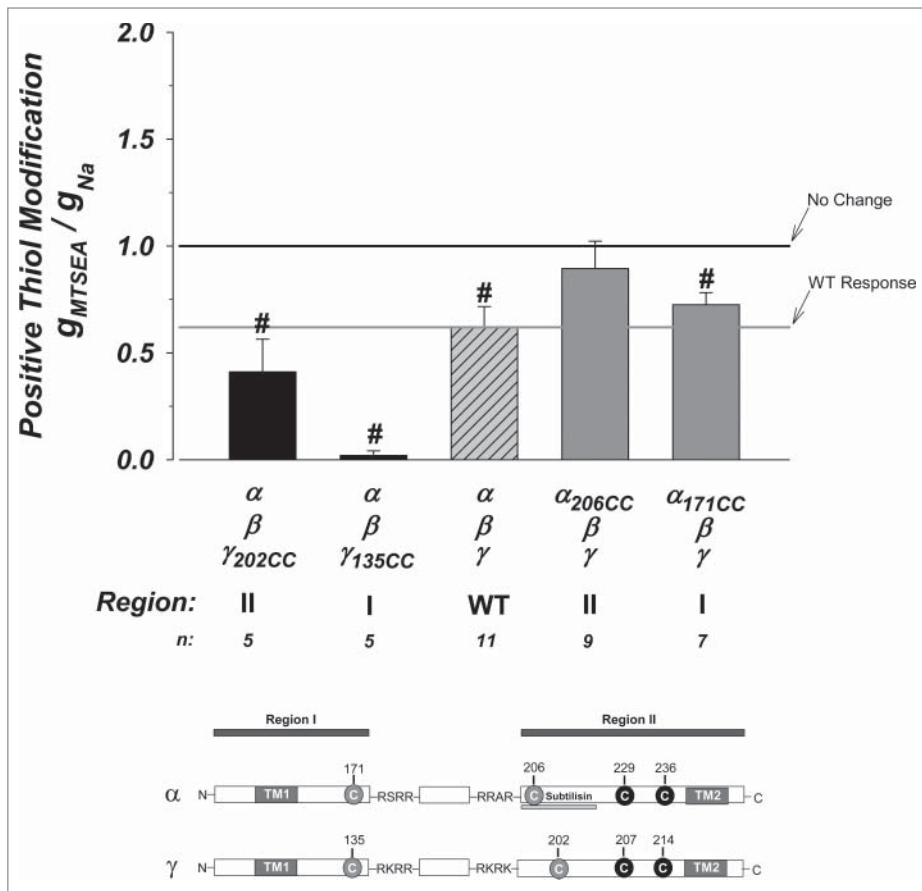


Figure 5. Effects of thiol modification on the cysteine mutant constructs. The thiol modifying reagent MTSEA was used to covalently introduce positive charges at free cysteines. The WT channel was inhibited by ~40% indicating availability of a free and accessible cysteine. Unpaired cysteines at γ region I and II were further inhibited from WT with that at γ region I inhibited by 98%. All other constructs were similar to WT indicating that the cysteines are not available for covalent charge modification or that modification does not contribute additional effects to those observed with the introduction of the exogenous cysteines. N = 5–11. See **Figure 3** legend for additional details.

Shown in **Figure 6** are the effects of positive charge modification in subtilisin cleaved channels. Comparing these effects to those summarized in **Figure 5** represents the differences between subtilisin versus furin cleaved channels. MTSEA's inhibition of the WT channel was not different between these groups. However, this does not only indicate that MTSEA blocked the WT channel to the same extent, but that it also abrogated the stimulation normally found by subtilisin treatment. This implies that the endogenous thiol which is modified in the ENaC subunits is within close 3-dimensional proximity to the region cleaved by subtilisin at a.a. 205–221. Interestingly, all predicted unpaired cysteines in α and γ are within such proximity (see Discussion).

The effects on γ region I was markedly different where MTSEA modification did not block subtilisin cleaved channels. Instead a 3-fold stimulation vs 0.98-fold inhibition was observed. This provides strong evidence that elimination of region 205–221 in α eliminated the site where MTSEA modified

cysteine in γ 135 interacted with. Thus, these data provide further evidence for the location of interaction between γ region I and α region II in the mature channel.

Interactions in region I in α exhibited an opposite effect where MTSEA modification lead to increased inhibition of subtilisin cleaved channels as compared to WT vs. no difference from WT when comparing furin cleaved channels. This also indicates that α 205–221 is a likely site of interaction as its elimination modified channel activity. This inverse effect would indicate a stabilizing effect of this interaction on the electrically active channel.

Discussion

We examined the interaction between the α and γ subunits in the trimeric Epithelial Na^+ Channel. We specifically examined the roles of the N- and C-terminal fragments, referred to as regions I and II, created in these subunits after cleavage by endogenous and exogenous proteases. Using cysteines engineered upstream and downstream of the cleavage zones in these subunits, we demonstrate the interaction of the untethered (post cleavage) region I of both α and γ with the mature channel. Further, those regions as well as γ region II, interacted with the N-terminus of region II in α to control activity. Some of these interactions were sensitive to

reduction and markedly compromised by insertion of positive charge, providing further insights into the location and mechanism of these interactions. Altogether, our results delineate regions in the proteolytically active channel that control activity and demonstrate functional roles of channel fragments in proteolytic activation. Given the low occurrence of α region I fragment at the membrane we propose that this may represent a rate limiting step to the observation of high activity channels.

Homology to ASIC and endogenous cysteines

The ASIC structure has been used to predict intra-subunit interactions in ENaC, e.g. to examine the roles of the wrist, palm and finger domains and the roles of homologous regions in ENaC in ion conduction and selectivity.⁶ However, as pointed out ASIC lacks critical ENaC features that preclude the use of this approach in assessing channel activation or cleavage. Foremost is the absence of cleavage sites and surrounding amino

acids, referred to as hypervariable region,⁶ from ASIC. For these and other reasons we introduced cysteine mutagenesis within the hypervariable region.

Outside of the hypervariable region homologous ENaC disulfides have been identified.²² These are limited to inter-subunit disulfides given the homomeric versus heteromeric nature of ASIC and ENaC. These include a disulfide in both α and γ which spans the hypervariable region and may tether region I to region II fragments. Our data favor an untethered configuration based on: 1) the lower density of the region I fragment at the membrane (see Figure 2 and Hu et al¹⁶) when examined with the same antibody directed against the same epitope, 2) the absence of marked channel activity disruption by reducing agents (Fig. 4) and 3) differences in the effects of modification of region I of α vs. γ .

Role of the γ fragments in channel activity

Modifications to both γ fragments diminished activity in the absence of effects on expression or cleavage. This provides the first evidence for a functional role of both fragments I and II of γ in mature channel function. The effects of these modifications on exogenous cleavage by subtilisin (Fig. 3) provided compelling evidence as to the role of these fragments in the mature channel. We were able to narrow sites of these interactions to the new N-terminus of region II α based on the attenuated response of these constructs to subtilisin, and the known position cleaved by subtilisin in α between a.a. 205 and 221.¹⁶ As we have shown before γ is already fully cleaved in this system and no further effects of subtilisin are observed on this subunit. This indicates that γ 135 and γ 202 interact with α between a.a. 205 and 221.

Modification of γ region I provided the strongest effect on exogenous channel activation by subtilisin. Further modification of this exogenous cysteine at γ 135 by positive charges resulted in near complete (98%) inhibition of channel activity (Fig. 5). This extensive inhibition was only observed with positive charge modification. This suggests a potential role of this site in γ along with the interacting site in α in charge selection and ion conduction. Subsequent elimination of a.a. 205–221 in α by exogenous subtilisin relieved the inhibition by positive charge leading to the observation of a nearly 3-fold stimulation, likely owing to the ability of subtilisin in cleaving uncleaved α subunits at the membrane (Fig. 6). Altogether, these results indicate that both regions

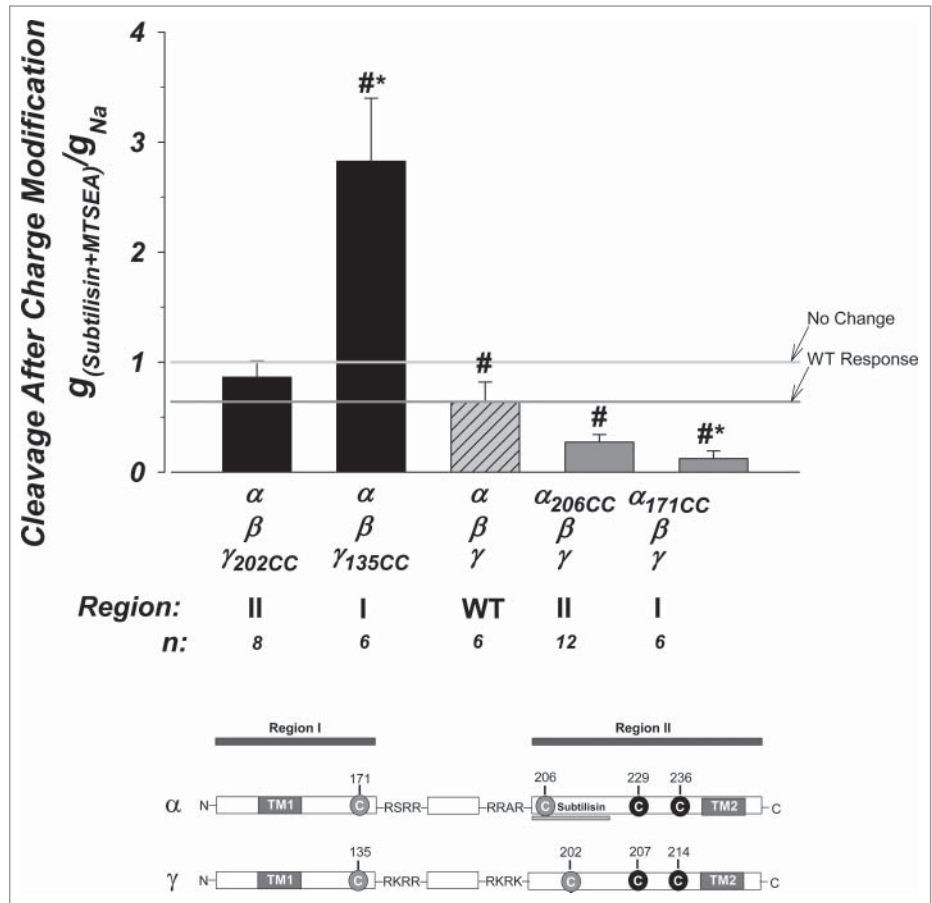


Figure 6. Effects of thiol modification are altered in subtilisin cleaved channels. The effects of positive charge modification were examined in subtilisin cleaved channels. Modification of the WT channel was similar to that observed in Figure 5 for furin cleaved channels and exhibited an ~40% inhibition. Modification to γ region II was not different from WT. However, positive charge modification to channels made with γ region I resulted in nearly 3-fold stimulation, in contrast to that observed to the furin cleaved channel in Figure 5. Those made with α region I was inhibited from the WT channel, in contrast to the no difference observed in Figure 5. These indicate marked differences in the interaction of these regions with the channel in the presence or absence of the tract between a.a. 205 and 221 in α region II (see text). N = 6–12. See Figure 3 legend for more details.

I and II in γ converge on the N-terminus of region II in α and that both fragments of γ are necessary for channel function.

Role of the α fragments in channel activity

Cysteine insertion in both α fragments also diminished endogenously cleaved channel activity in the absence of effects on expression and processing. The effects of modification on α 206 in region II are understandable in light of the effects above observed with γ -reduced ability of this construct to interact with γ regions I and II results in an inhibition. This is supported by the results of Figure 3 showing nearly 3-fold stimulation of α 206 versus WT channel by subtilisin as this exogenous protease would cleave downstream of the exogenous cysteine, thus releasing this cysteine and relieving the 2.5-fold inhibition of baseline activity (Fig. 1).

Our results also support a role of α region I in mature channel activity in both furin and subtilisin cleaved channels. Indeed

α 171 inhibited baseline activity and this effect was not significantly changed following cleavage by subtilisin. This exogenous cysteine however, stabilized the channel in response to reduction by TCEP indicating that it is likely paired with an endogenous cysteine forming a disulfide bridge. This was consistent with the absence of additional thiol modification of this construct.

Interestingly, the effects of positive charge thiol modification in α region I were markedly modified following subtilisin cleavage (Fig. 6) leading to inhibition of activity. The simplest explanation is that α 171 also interacts with the mature channel close to the subtilisin cleavage site and that this interaction may possibly utilize one of the 2 predicted free cysteines in this region (Fig. 7). In this case elimination of the interference from the tract in α between 205–221 renders the cysteine at α 171 unpaired and free to be modified by thiols. Following positive charge modification a larger inhibition is observed. Thus, both regions I of α and γ may interact with α region II to determine charge selection and ion conduction.

Role of the N-termini/mechanism of activation by cleavage

We have previously proposed that channel rearrangement occurs after cleavage and that this rearrangement is more favorable to channel-lipid bilayer hydrophobic thickness leading to an increase of activity. This is supported by numerous studies where:

(1) the elimination of the so called “inhibitory domain” in the absence of cleavage did not stimulate the channel, (2) the much lower density of the N-terminal fragment at the membrane (see Fig. 2), (3) the presence of multiple mechanisms that affect lipid bilayer fluidity that can increase activity and open probability in the absence of changes to cleavage,¹⁷ and (4) the insensitivity of the exact cleavage site where multiple proteases with varying specificities can lead to the same type of activation.¹⁶

Our data indicate that region II in α ENaC downstream of the 2nd furin cleavage site is a “hotspot” for channel interaction with the remaining subunit fragments, and we find a marked change in the accessibility to thiol modification after subtilisin’s cleavage in this “hotspot.” These results demonstrate major structural channel rearrangement after just a single cleavage event by subtilisin in α ENaC. Given our recent demonstration of multiple open channel states,¹⁷ changes in channel bilayer interactions or stability after cleavage remain the best likely explanation.

How do we reconcile our current data demonstrating a clear role of region I in both α and γ with our previous data indicating the disappearance of these fragments from the membrane? We propose that these structural rearrangements are a likely rate limiting step to the observation of a functional electrically active channel. Our data using the same tag in different parts of the subunit

are the only ones which can address the question of fragment levels at the membrane, as the same antibody can be utilized to examine the levels of all fragments. The N-termini of the cleaved subunits do indeed disappear from the membrane as we have previously reported¹⁶ and as evident from the example blot in Figure 2 which demonstrates the absence of comparable expression of HA tagged region I and II α ENaC (24 kDa vs. 60 kDa fragments). This is likely because of the presence of consensus sites for ubiquitination in the N-terminus²³ resulting in internalization or degradation of the majority of region I protein. However, the decrease of these termini to levels near the limit of Western Blot detection does not mean the complete disappearance from the membrane, and indeed in the face of such major structural rearrangement it would be expected to be a highly inefficient process where only those fragments that are successful in forming a mature channel yield electrical activity, while those which are not, remain separate and are internalized. Further, the efficiency of such a process may also be cell type dependent.

Accordingly, and consistent with the current and previous observations we propose that the presence of the intact

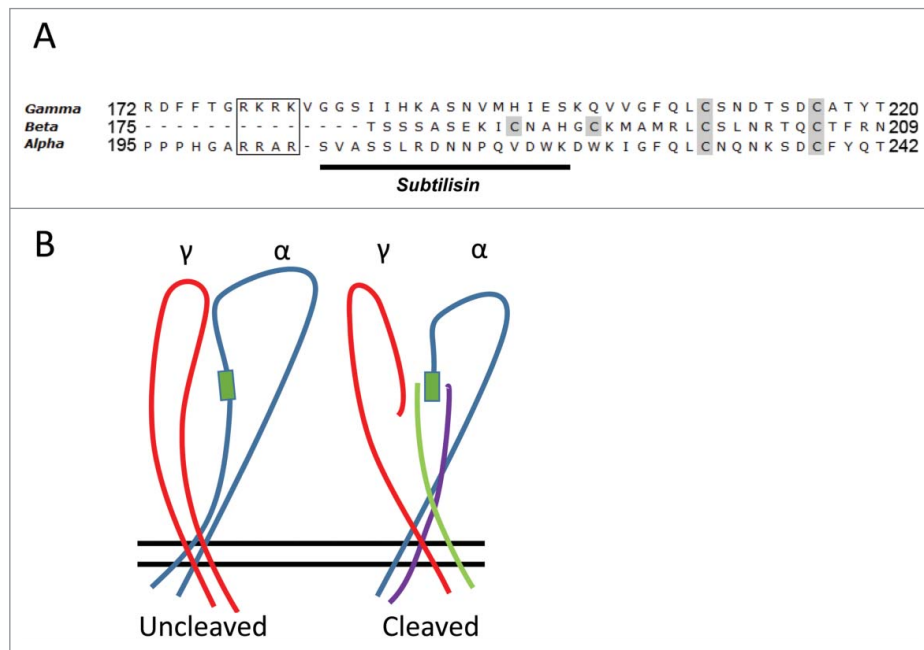


Figure 7. Endogenous Cysteines and simplified model of interaction. (A) Sequence alignment of the ENaC subunits downstream and including the second cleavage site in α and γ (boxed). Shown in gray are cysteines predicted to be free from homology modeling to the ASIC crystal structure. The 4 free cysteines in α and γ cluster within 35 a.a. of the 2nd cleavage site. The remaining 4 free cysteines in β cluster within the homologous comparable region in this subunit; which lacks cleavage sites. Solid underline shows subtilisin cleavage tract in α . (B) Simplified model depicting extracellular loops of α and γ (β is eliminated for clarity). This model illustrates the interactions in α and γ fragments I and II predicted from the current work. The left image represents pre-cleavage α (blue) and γ (red) while that on the right illustrates how post cleavage γ region II (red), α region II (blue), interact with γ region I (green) and α region I (purple). These interactions occur in the region defined by subtilisin cleavage in α (green box).

uncleaved stretch of amino acids between regions I and II inhibit the interaction between region I in α and γ and region II in α . This inhibition is relieved by generic cleavage in the general vicinity of the furin sites, allowing untethering of regions I in α and γ and permitting the interactions uncovered in the present work to occur. This also may occur at lower efficiency due to the internalization of the presumably ubiquitinated N-terminal fragments. It has been shown that surface expression of this fragment in rat increases in response to a low sodium diet,²⁴ consistent with this interpretation and suggesting regulated internalization of this fragment. Additional experimental approaches are needed to further test this hypothesis.

Materials and Methods

Constructs

Constructs utilized HA-tagged (α) or untagged (β and γ) vectors containing inserts previously described.¹⁶ The cysteine mutants were introduced at each location by conventional mutagenesis (Genscript Inc., Piscataway, NJ). These double cysteines were placed to bracket the identified furin cleavage sites in α ENaC; where the underlined sequence was replaced by cysteines at α 171VAGSRSR and α 201RRARSVA to α 171CCGSRSR and α 201RRARSCC. In γ ENaC the sequences flanking the 2 cleavage sites at γ 135SRKRR and γ 178RKRKVGG were converted to γ 135CCSRKRR (insertion) and γ 178RKRKVCC. A third site at γ 202VG was converted to γ 202CC (see Fig. 1A).

Two adjacent cysteines are unfavorable to form a disulfide,²⁵ and the use of double cysteines increases the likelihood of external modification. The third site in γ outside the identified cleavage tract was selected to determine if there are differences in mutations immediately next to the terminal furin site and downstream from that. This was not possible in α due to the interference with subtilisin's cleavage which was a critical part of our approach.

RNA

Purified DNA plasmids were linearized and then in vitro transcribed with the T7 Ribomax Large Scale RNA Production Kit (Promega, Madison, WI) using 5-fold excess of methylated GTP Cap analog (New England Biolabs, Ipswich, MA). At the termination of the reaction, the contents were treated with DNase I (Promega) and purified by phenol/chloroform extraction and ethanol precipitation. Capped RNA concentrations were initially determined by UV spectroscopy and then validated by gel electrophoresis and adjusted if necessary to assure identical concentrations were injected. cRNA for all constructs were injected at a final concentration of 2.5 ng per oocyte.

Xenopus oocytes

Frogs were obtained from *Xenopus* Express (Brooksville, FL). Oocytes were surgically excised from ovarian lobes of HCG pre-injected frogs. Oocytes were defolliculated by digestion with type IA collagenase (Sigma-Aldrich, St. Louis MO) in Ca²⁺ free OR2 medium.²⁶ Following defolliculation, stage V and VI oocytes

were selected and allowed to recover overnight in ND94 (94 mM NaCl, 1 mM MgCl₂, 1.8 mM CaCl₂, 2 mM KCl, 5 mM HEPES, pH 7.4) containing 1% of 10,000 U penicillin-streptomycin (Mediatech, Corning NY) and 50 μ g/ml amikacin (MP Biomedicals, Solon OH) at 18°C. Oocytes were injected with cRNAs for all 3 ENaC subunits. All recordings were carried out 1–3 d post injection. Homogenization for SDS-PAGE/Western Blot occurred 2–3 d post injection.

Two electrode voltage clamp

Measurement, calculation, and recording of oocyte membrane conductance and capacitance were carried out as previously described.²⁷ In brief, oocytes were clamped to a holding potential of 0 mV with a TEV-200 voltage clamp (Dagan Instruments, Minneapolis MN) to eliminate voltage induced Na⁺ loading artifacts and rundown. Slope conductance at the holding potential was measured in 10s intervals and membrane conductance was calculated as previously described.²⁷ Agar/AgCl electrodes were used to protect against flow or redox caused artifacts as previously described.²⁸ The recording medium was identical to the storage medium except for the absence of antibiotics. All experiments utilized amiloride (Merck, Rahway NY) at 10 μ M to assess the whole cell ENaC component and the amiloride sensitive conductance; g_{Na} . All groups were recorded on all days to allow normalization and intergroup comparisons.

Western blot

To account for inherent variations between oocytes from different frogs and batches of oocytes, Western Blots were carried out 3–7 times and the data represent the summary of these experiments. Western blots were carried out as described previously.¹⁷ Briefly, 50 oocytes per group were biotinylated with EZ-Link Sulfo-NHS-SS-Biotin (Thermo Scientific, Rockford IL) on ice and then extensively washed and homogenized by a ground glass homogenizer. Biotinylated membrane proteins were pulled down with streptavidin-agarose beads (Thermo Scientific). To release the bound proteins, samples were heated at 65°C for 20 minutes, spun down and loaded and separated by SDS-PAGE and transferred to nitrocellulose membranes. Membranes were probed with an anti-HA antibody (clone 3F10, Roche Life Sciences, Indianapolis IN), or a previously described antibody developed against an epitope in the γ extracellular loop.²⁹ Membranes were visualized with enhanced chemiluminescence HRP substrate (SuperSignal Dura West Extended Duration Substrate, Thermo Scientific) in a gel documentation system (MP4000, BioRad Hercules Ca) and analyzed with the included imaging software (Image Lab).

Amidolytic assay

Subtilisin activity was assayed as previously described for other ENaC substrates.²⁹ Briefly, peptides containing identified α and γ ENaC cleavage sites (RTAR, RKRR, RKRK) were synthesized and coupled at their C-terminus to amino-methylcoumarin (Genscript Inc.). The amide bond (peptide-coumarin) quenches coumarin's fluorescence and this is relieved by proteolysis at the terminal amino acid. This reaction is assayed fluorometrically at an excitation/

emission wavelength of 360/460 nm to yield cleavage reaction velocities (V). Maximal or initial velocity (V_{max}) was determined at 37°C in a 96 well plate reader (Bio-Tek Instruments, Winooski, VT).

Reagents

TCEP was obtained from Gold Biotechnology (St. Louis, MO). MTSEA and MTSES were obtained from Affymetrix (Santa Clara, CA). Proteases (subtilisin A type VIII from *Bacillus Licheniformis*, and trypsin type I from bovine pancreas) were obtained from Sigma-Aldrich (St. Louis, MO).

Protease and redox protocols

ENaC expressing oocytes were treated with the serine protease subtilisin or trypsin at a concentration of 50 ng/ml for 15 minutes. The degree of activation was calculated as the ratio of the amiloride sensitive conductance after and before proteolysis. TCEP was used at 500 μ M, H₂O₂ at 10 mM

and the MTS reagents at 1 mM. All treatments were done for 15 minutes.

Significance was determined at $P < 0.05$ by Student's t-test or one sample t-test as appropriate and as indicated in the figures.

Disclosure of Potential Conflicts of Interest

No potential conflicts of interest were disclosed.

Funding

This work was supported by NIH grant DK55626 and by the John R. Oishei Foundation.

Supplemental Material

Supplemental data for this article can be accessed on the publisher's website.

References

- Abriel H, Loffing J, Rebhun JF, Pratt JH, Schild L, Horisberger J-D, Rotin D, Staub O. Defective regulation of the epithelial Na⁺ channel by Nedd4 in Liddle's syndrome. *J Clin Invest* 1999; 103:667; PMID:10074483; <http://dx.doi.org/10.1172/JCI5713>
- Canessa CM, Horisberger JD, Rossier BC. Epithelial sodium channel related to proteins involved in neurodegeneration. *Nature* 1993; 361:467-70; PMID:8381523; <http://dx.doi.org/10.1038/361467a0>
- Canessa CM, Schild L, Buell G, Thorens B, Gautschi I, Horisberger JD, Rossier BC. Amiloride-sensitive epithelial Na⁺ channel is made of three homologous subunits. *Nature* 1994; 367:463-7; PMID:8107805; <http://dx.doi.org/10.1038/367463a0>
- Lingueglia E, Voilley N, Waldmann R, Lazdunski M, Barbry P. Expression cloning of an epithelial amiloride-sensitive Na⁺ channel. A new channel type with homologies to Caenorhabditis elegans degenerins. *FEBS Lett* 1993; 318:95-9; PMID:8382172; [http://dx.doi.org/10.1016/0014-5793\(93\)81336-X](http://dx.doi.org/10.1016/0014-5793(93)81336-X)
- Jasti J, Furukawa H, Gonzales EB, Gouaux E. Structure of acid-sensing ion channel 1 at 1.9 Å resolution and low pH. *Nature* 2007; 449:316-23; PMID:17882215; <http://dx.doi.org/10.1038/nature06163>
- Stockand JD, Staruschenko A, Pochynyuk O, Booth RE, Silverthorn DU. Insight toward epithelial Na⁺ channel mechanism revealed by the acid-sensing ion channel 1 structure. *IUBMB Life* 2008; 60:620-8; PMID:18459164; <http://dx.doi.org/10.1002/iub.89>
- Kashlan OB, Kleyman TR. ENaC structure and function in the wake of a resolved structure of a family member. *Am J Physiol Renal Physiol* 2011; 301:F684-F96; PMID:21753073; <http://dx.doi.org/10.1152/ajprenal.00259.2011>
- McDonald FJ, Price MP, Snyder PM, Welsh MJ. Cloning and expression of the beta- and γ -subunits of the human epithelial sodium channel. *Am J Physiol* 1995; 268(5 Pt 1):C1157-63; PMID:7762608
- Hughey RP, Bruns JB, Kinlough CL, Harkleroad KL, Tong Q, Carattino MD, Johnson JP, Stockand JD, Kleyman TR. Epithelial sodium channels are activated by furin-dependent proteolysis. *J Biol Chem* 2004; 279:18111-4; PMID:15007080; <http://dx.doi.org/10.1074/jbc.C400080200>
- Hughey RP, Mueller GM, Bruns JB, Kinlough CL, Poland PA, Harkleroad KL, Carattino MD, Kleyman TR. Maturation of the epithelial Na⁺ channel involves proteolytic processing of the alpha- and γ -subunits. *J Biol Chem* 2003; 278:37073-82; PMID:12871941; <http://dx.doi.org/10.1074/jbc.M307003200>
- Vallet V, Chraïbi A, Gaeggeler HP, Horisberger JD, Rossier BC. An epithelial serine protease activates the amiloride-sensitive sodium channel. *Nature* 1997; 389:607-10; PMID:9335501; <http://dx.doi.org/10.1038/39329>
- Chraïbi A, Vallet V, Firsov D, Hess SK, Horisberger JD. Protease modulation of the activity of the epithelial sodium channel expressed in *Xenopus* oocytes. *J Gen Physiol* 1998; 111:127-38; PMID:9417140; <http://dx.doi.org/10.1085/jgp.111.1.127>
- Caldwell RA, Boucher RC, Stutts MJ. Serine protease activation of near-silent epithelial Na⁺ channels. *Am J Physiol Cell Physiol* 2004; 286:C190-4; PMID:12967915; <http://dx.doi.org/10.1152/ajpcell.00342.2003>
- Carattino MD, Sheng S, Bruns JB, Pilewski JM, Hughey RP, Kleyman TR. The epithelial Na⁺ channel is inhibited by a peptide derived from proteolytic processing of its alpha subunit. *J Biol Chem* 2006; 281:18901-7; PMID:16690613; <http://dx.doi.org/10.1074/jbc.M604109200>
- Bruno JB, Carattino MD, Sheng S, Maarouf AB, Weisz OA, Pilewski JM, Hughey RP, Kleyman TR. Epithelial Na⁺ channels are fully activated by furin- and prosta-sin-dependent release of an inhibitory peptide from the γ -subunit. *J Biol Chem* 2007; 282:6153-60; PMID:17199078; <http://dx.doi.org/10.1074/jbc.M610636200>
- Hu JC, Bengrine A, Lis A, Awayda MS. Alternative mechanism of activation of the epithelial na⁺ channel by cleavage. *J Biol Chem* 2009; 284:36334-45; PMID:19858199; <http://dx.doi.org/10.1074/jbc.M109.032870>
- Berman JM, Brand C, Awayda MS. A Long Isoform of the epithelial sodium channel alpha subunit forms a highly active channel. *Channels* 2014; 9(1):30-43.
- Ruffieux-Daidié D, Staub O. Intracellular ubiquitylation of the epithelial Na⁺ channel controls extracellular proteolytic channel activation via conformational change. *J Biol Chem* 2011; 286:2416-24; PMID:21084303; <http://dx.doi.org/10.1074/jbc.M110.176156>
- Gosalia DN, Salisbury CM, Ellman JA, Diamond SL. High throughput substrate specificity profiling of serine and cysteine proteases using solution-phase fluorogenic peptide microarrays. *Mol Cell Proteomics* 2005; 4:626-36; PMID:15705970; <http://dx.doi.org/10.1074/mcp.M500004-MCP200>
- Kuner T, Wollmuth LP, Karlin A, Seeburg PH, Sakmann B. Structure of the NMDA receptor channel M2 segment inferred from the accessibility of substituted cysteines. *Neuron* 1996; 17:343-52; PMID:8780657; [http://dx.doi.org/10.1016/S0896-6273\(00\)80165-8](http://dx.doi.org/10.1016/S0896-6273(00)80165-8)
- Dunten RL, Sahin-Toth M, Kaback HR. Role of the charge pair aspartic acid-237-lysine-358 in the lactose permease of *Escherichia coli*. *Biochemistry* 1993; 32:3139-45; PMID:8457574; <http://dx.doi.org/10.1021/bi00063a028>
- Zha X-M, Wang R, Collier DM, Snyder PM, Wemmie JA, Welsh MJ. Oxidant regulated inter-subunit disulfide bond formation between ASIC1a subunits. *Proc Natl Acad Sci* 2009; 106:3573-8; PMID:19218436; <http://dx.doi.org/10.1073/pnas.0813402106>
- Staub O, Gautschi I, Ishikawa T, Breitschopf K, Ciechanover A, Schild L, Rotin D. Regulation of stability and function of the epithelial Na⁺ channel (ENaC) by ubiquitination. *EMBO J* 1997; 16:6325-36; PMID:9351815; <http://dx.doi.org/10.1093/emboj/16.21.6325>
- Frindt G, Ergonul Z, Palmer LG. Surface expression of epithelial Na channel protein in rat kidney. *J Gen Physiol* 2008; 131:617-27; PMID:18504317; <http://dx.doi.org/10.1085/jgp.200809989>
- Park C, Raines RT. Adjacent cysteine residues as a redox switch. *Protein Eng* 2001; 14:939-42; PMID:11742114; <http://dx.doi.org/10.1093/protein/14.11.939>
- Awayda MS. Regulation of the epithelial Na⁺ channel by membrane tension. *J Gen Physiol* 1998; 112:97-111; PMID:9689021; <http://dx.doi.org/10.1085/jgp.112.2.97>
- Awayda MS. Specific and nonspecific effects of protein kinase C on the epithelial Na⁺ channel. *J Gen Physiol* 2000; 115:559-70; PMID:10779314; <http://dx.doi.org/10.1085/jgp.115.5.559>
- Berman JM, Awayda MS. Redox artifacts in electrophysiological recordings. *Am J Physiol Cell Physiol* 2013; 304:C604-13; PMID:23344161; <http://dx.doi.org/10.1152/ajpcell.00318.2012>
- Awayda MS, Awayda KL, Pochynyuk O, Bugaj V, Stockand JD, Ortiz RM. Acute cholesterol-induced anti-natriuretic effects: role of epithelial Na⁺ channel activity, protein levels, and processing. *J Biol Chem* 2011; 286:1683-95; PMID:21041305; <http://dx.doi.org/10.1074/jbc.M110.159194>